



EXPERIMENTS DIVISION

Doc. Nr.	EDMS	Created	Printed	Pages	Revision
EXD-BL04-GD-0002		2007-05-07	2007-05-25	11	3

Addendum to the Conceptual Design Report of the Materials Science and Powder diffraction beam line MSPD at ALBA

ABSTRACT

This addendum describes the changes to the original optical design of the MSPD beamline (BL04) described in EXD-BL04-GD-0001.

Prepared by	Checked by	Approved by
Michael Knapp and Inma Peral		
Distribution list		

Contents

1	SCOPE OF THE DOCUMENT	3
2	MAIN OPTICAL COMPONENTS	3
3	LAYOUT OF OPTICAL COMPONENTS: DISTANCES AND FOCAL LENGTHS	4
4	WORKING CONFIGURATIONS OF THE OPTICAL ELEMENTS	4
4.1	MIRRORED MODE	5
4.2	UN-MIRRORED MODE	5
5	EXPECTED BEAM LINE PERFORMANCE	5
5.1	HEAT LOADS IN OPERATING CONDITIONS	5
5.2	HEAT LOAD EFFECTS ON OPTICAL ELEMENTS, SLOPE ERROR	8
5.2.1	<i>Heat load on collimating mirror</i>	8
5.2.2	<i>Heat load on the 1st monochromator crystal</i>	9
5.3	ESTIMATION OF THE OPTICAL CHARACTERISTICS OF THE COLLIMATING MIRROR	9
5.3.1	<i>Slope error</i>	9
5.3.2	<i>Surface roughness</i>	10
6	VERTICAL BEAM POSITIONS AND BEAM SIZES	10
7	PRELIMINARY FLOOR LAYOUT	11
8	REFERENCES	11

1 Scope of the document

This addendum describes the changes to the original optical design of the MSPD beamline (BL04). The main changes are i) the suppression of the 2nd mirror M2, ii) the replacement of the channel cut monochromator by a double crystal monochromator and iii) the reduction of the horizontal aperture of the beam.

The new design slightly modifies the accent of the beamline leading to the following main consequences:

- The suppression of the 2nd mirror simplifies alignment and operation of the beamline but, above all, avoids negative influence on the reflection profiles of the powder diffraction pattern produced by the mirror, which is favored over a gain in intensity.
- The double crystal monochromator will reduce the contamination from Laue spots which are particularly problematic for spatially large beams that are produced by broad energy band sources (e.g. wigglers and bending magnets) [Kostroun80, webpage].
- And, finally, the reduction of the horizontal aperture provides an adequate beam size at both experimental stations and at the same time reduces considerably the heat load on the optical elements.

The implications of this changes on the optical layout and heat loads are described hereafter.

2 Main optical components

Filters

The optical elements are preceded by a variable white beam filter to strip off the low energy part of the wiggler spectrum and reduce the heat load on the downstream optics. Due to the high heat load the vacuum window upstream the optics also has to be protected by a preceding filter (the pre-filter). Depending on the final design it might be composed of two filter elements: pre-filter1 and pre-filter 2.

First mirror M1

The first mirror M1 will be installed to i) reduce the heat load on the monochromator ii) suppress higher harmonics and iii) collimate the beam in the vertical direction, thus increasing the energy resolution. This is necessary in order to achieve high resolution powder diffraction data.

Monochromator

The monochromator will produce a monochromatic beam with dE/E of about $2 \cdot 10^{-4}$ in the 7 – 50keV range. The crystals receive high heat load, thus adequate cooling must be provided. The design should be realized in a Double Crystal Monochromator setup (DCM) using one pair of Si111 crystals and with the following approximated dimensions:

1 st crystal: LxWxH:	110x30x50mm ³
2 nd crystal: LxWxH:	250x30x20mm ³
Gap:	10mm
Beam Offset:	~20mm

Focusing KB system with multilayers

The KB system provides focusing on station 1, SC/HP, for energies > 20keV. The mirrors will be covered by multilayers offering a wide variety in beam conditioning up to 80keV. A double layer spacing of about 3nm with lateral grading is proposed. The length of each mirror is 300mm and they will be mounted in a mechanical bender.

3 Layout of optical components: distances and focal lengths

The preliminary positions of the optical elements are:

ID center:	0m
Gate valve of front end (FE):	18.2m
M1 collimating mirror:	20m
DCM monochromator:	23m
End of Optics Hutch	27m
KBV:	29.5m
KBH:	29.9m
HP / SC station 1:	32m
PD station 2:	35m
End of Experimental Hutch	38m
Mirror glancing angle:	2mrad

4 Working configurations of the optical elements

The reflectivity of the mirror coating restricts the accessible energy range. The coating materials are chosen to cover the range between 8 – 40keV with a constant angle of 2mrad for the mirror.

Therefore, we plan for two main configurations of the optical elements:

Mirrored mode: 8 - 40keV.

Un-mirrored mode: > 40keV

In both modes the KB-multilayer mirror can be used as additional focusing option. The KB-mirror will be placed 2.1 to 2.5m upstream station 1 focusing the beam between 20 and 50keV, thus covering the high energy region for HP experiments.

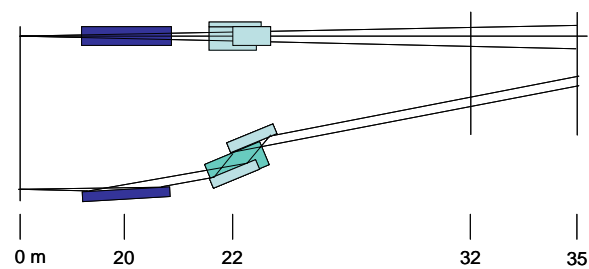


Figure 3.1 (I) Mirrored mode E_{phot} : 8 - 40keV

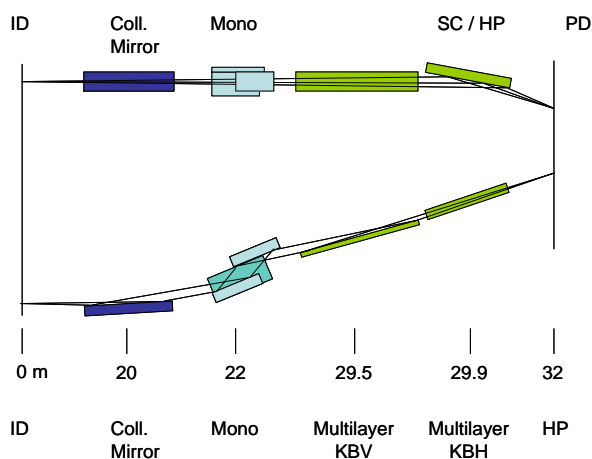


Figure 3.2 (II) Mirrored mode with multilayer KB-optics, E_{phot} : 20 - 40keV

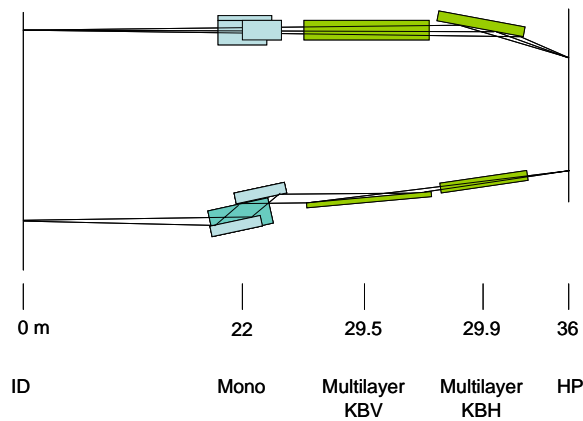


Figure 3.3 (III) Un-mirrored mode with multilayer KB-optics, $E_{\text{phot}} > 40\text{keV}$.

(IV) Un-mirrored mode without secondary optics is not shown. $E_{\text{phot}} > 40\text{keV}$

4.1 Mirrored mode

The energy range in the mirrored mode is defined by the mirror coating and grazing angle. To cover a wide energy range without the need of major realignments the mirrors will be operated at a fixed glancing angle of 2mrad. In the mirrored mode a bendable collimating mirror upstream the monochromator is inserted into the beam path. Three different coatings (Si, Rh, Pt or Ir) on the collimating pre-mirror adapt for the different energy ranges. The small angle of the collimating mirror allows for a liquid metal contacted external cooling with the cooling pipes in a GaIn (Galinstan) filled bathtub. At the PD station the beam has an angle of 4mrad in the vertical direction.

The mirrored mode, will serve about 80% of the applications and is also standard setup for powder diffraction.

4.2 Un-mirrored mode

The un-mirrored mode is used for high energy applications around 50keV. For energies above the transmitted range of the mirror the monochromator can directly be operated in the beam. As this is a high energy (high K-value) setting the white beam slits have to be set to a reasonably small value. In this configuration the KB-system will be used as focusing device.

5 Expected beam line performance

5.1 Heat loads in operating conditions

A very important issue at this beam line is the accepted total power and power density in the optical components. In particular three parameters define heat load and flux transferred to the optics: apertures, transmittance of filters and K-value of the source. The usable range of these parameters is determined by the maximum heat load that the optical elements can handle. Typical values and the usable ranges of these parameters are presented below.

Vertical aperture:

The vertical aperture is defined by the acceptance of the collimating mirror which is typically 125 μrad (1.2m mirror length @ 2mrad grazing angle) resulting in 2.4mm beam height.

The vertical aperture in the un-mirrored high energy setting is defined by either the acceptance of the monochromator and multilayer optics, the vertical beam size at the sample position or the acceptable heat load on the first monochromator crystal. The latter

can of course be adapted by the white beam filters. The aperture in the un-mirrored setup always stays below the value of the mirrored beam.

Horizontal aperture:

Due to heat load, acceptance of the downstream KB-mirror and the horizontal beam size at the sample position, the horizontal aperture under working conditions is restricted to a maximum of 400 μ rad. In most cases an acceptance of 200 μ rad will be sufficient (see tables 4.1, 4.2 and 4.3).

Filters and vacuum windows

Two different ways to separate the beam line from the front-end (FE) and storage ring vacuum are possible: The conventional way by using a Be-window and if necessary Be or graphite pre-filters and alternatively CVD-diamond windows of about 0.3mm thickness, that are increasingly employed at sources like ESRF for undulator beams. A third, mirrorless variant employing differential pumping is not relevant, since the thereby accessible low energy region is not needed at this beam line.

A solution with Be vacuum-window and Pyrographite or CVD-diamond pre-filter is preferred, followed by a variable white beam filter box.

Absorbed power on mirror

Due to the small glancing angle the fraction of the total power passing through the aperture and being absorbed in the pre-mirror is rather low. Besides, the power absorbed in the pre-mirror depends on the selected coating material and thus on the energy range. In all cases considered the maximum absorbed power can be kept below 1.1kW.

Absorbed power on monochromator

Both monochromator crystals will be externally cryo-cooled to reduce the influence of thermally induced distortion. Literature addressing this problem report different values for acceptable heat loads and propose different cooling schemes (e.g. Tajiri01, Zhang03, Chumakov04). One of the most optimistic estimations is given by Chumakov: "indirectly cooled silicon monochromators can provide an ideal performance up to a heat load of 400W and an acceptable performance at 900W". In his analysis no influence on the Si 111 reflection at 14.4keV was found up to a heat load of 900W.

Source Power Density

Table 4.1: Power density in normal incidence [W/mm^2] of the ID with no filtering. Only some values are exemplarily given.

Distance to ID (m)		18	19.5	20.5	21.5
K: 6.08	400mA	138	118	106	97
K: 6.08	250mA		73.8		
K: 3.65	400mA		70.6		
K: 3.65	250mA		44.2		

Heat loads on the optical components

Power absorbed by the optical components has been calculated for a number of representative conditions and are summarized in the following tables (table 4.2 – 4.5). Some extreme but realistic configurations are marked in yellow. Critical values, that means technically too difficult or with non-acceptable performance, are marked in red.

Table 4.2, 4.3, 4.4 and 4.5 abbreviations:

Apert: Power passing through aperture

C: Pyrographite filter (with thickness in mm)

D: Diamond filter

Be: Beryllium window

Si, Rh, Pt: Mirror with respective coating

Mono: 1st monochromator crystal

K	H _{Div} [μrad]	ID total	Apert	C0.3	C1.0	D0.4	Be0.3	C1.0	C3.0	C4.0	Si	Mono	Rh	Mono	Pt	Mono
3.65	300	4280	581	180	118		6				154	124	36	242	30	248
	400	4280	758	236	154		7.4				198	162	46	314	39	322
	600	4280	1111	355	228		11	-	-	-	280	237	64	454	54	463
	1000	4280	1693	592	354		16	-	-	-	374	358	81	651	73	659
6.08	300	11877	973	166	149		10				485	162	203	444	142	506
	400	11877	1275	218	195		13				635	213	266	583	186	663
	600	11877	1897	328	292		19	-	--	--	939	319	390	862	272	986
	600	11877	1897	328	292		19	159	288	-	709	102	316	495	211	600
	1000	11877	3079	550	483		32	260	468	359	859	71	401	529	261	669

Table 4.2: Phase 1: Synchrotron beam current $I = 250\text{mA}$, $V_{\text{Div}} = 122\mu\text{rad}$, absorbed power in the respective element given in Watt.

K	H	ID	Apert	C0.3	C1.0	D0.4	Be0.3	C1.0	C1.5	C3.0	C4.0	Si	Mono	Rh	Mono	Pt	Mono
3.65	300	6850	917	284	447		9									47	391
	400	6850	1213	378	246		12					317	259	74	502	62	514
	600	6850	177	568	364		17					448	380	102	726	84	741
4.08	200	11844	792			240	12					331	210				
	400	11844	1572			480	23					651	419				
6.08	200	19000	1017			239	14									158	606
	200	19000	1017			239	14										
	300	19000	1524	260	233		15					762	254	320	695	225	791
	300	19000	1524	260	233		15		176							203	636
	400	19000	2040	349	313							1027	350	429	949	300	1078
	400	19000	2040	349	313		21	170		310		769	109	345	532	231	646
	400	19000	2040			483	28					1068	460	443	1086	313	1216
	600	19000	3026	525	468		31	254		461	357	872	69	416	525	273	669

Table 4.3: Phase 2: Synchrotron beam current $I = 400\text{mA}$, $V_{\text{Div}} = 122\mu\text{rad}$, absorbed power in the respective element given in Watt.

K	H	ID	Apert	D0.3	D0.3	Be0.3	C1.0	C3.0	C4.0	Si	Mono	Rh	Mono	Pt	Mono
6.08	300	19000	1524	316	111	-	-	-	-	791	305	331	765	223	863
	400	19000	2040	125	150	-	346	-	-	914	205	393	726	269	850

Table 4.4: Phase 2: Synchrotron beam current $I = 400\text{mA}$, $V_{\text{Div}} = 122\mu\text{rad}$, absorbed power in the respective element given in Watt using diamond filters:

	H_{Div}	V_{Div}	ID	Apert	C0.3	C1.0	Be0.3	Mono
6.08	60	120	19000	294	50	45	3	197

Table 4.5: Phase 2: Synchrotron beam current $I = 400\text{mA}$, $V_{\text{Div}} = 120\mu\text{rad}$, absorbed power in the respective element for the 50keV case with KB-mirror:

Absorbed power densities in filter elements in worst case, $K=6.08$, $I=400\text{mA}$:

Pre-filter 1 (0.3mm Pyrographite)	18.6 W/mm ²
Pre-filter 2 (1.0mm Pyrographite)	17.1 W/mm ²
Be vacuum window	1.2 W/mm ²
First white beam filter (1mm Pyrographite):	9.5 W/mm ²

Pre-filter 1 (0.4mm Diamond @18m):	30.7 W/mm ²
Be vacuum window:	1.9 W/mm ²
First white beam filter (1mm Pyrographite @19m):	13.8 W/mm ²

Incoming Power density after 0.4mm diamond + 0.3mm Be @19m: 95W/mm²

5.2 Heat load effects on optical elements, slope error

FEA calculations were performed to estimate the thermal influence on the surface slope. Several realistic cases were considered.

5.2.1 Heat load on collimating mirror

Si coating

The Si coated mirror stripe absorbs almost three times more heat than the Pt stripe. Although the collimation requirements are more relaxed in the low energy region, this is assumed as a worst case.

The values for calculation are:

$K=4.8$ ($E_c=10\text{keV}$), 400mA Synchrotron current,

Aperture HxV: 400x125 μrad^2

Filter: 0.4mm CVD-Diamond, 0.3mm Be

Mirror angle: 2mrad

Total absorbed power: 664W

Peak power density: 0.07895W/mm²

Beam footprint HxV 8x1230mm²

Mirror dimension WxHxL: 140x70x1250mm³

Convective heat transfer coefficient:	9000W/m ² K
T _{water}	22°C
T _{Max}	30.9°C
Thermal conductivity of contact material Galinstan:	16.5 W/mK
Meridional slope error over optical length (not corrected):	+4.5μrad
Sagittal slope error over optical length (not corrected):	+7μrad

The effects of 664W absorbed power will mostly be compensated by changing the curvature of M1 (similarly to the heat load effect described in CDR, section 4.3.1).

5.2.2 Heat load on the 1st monochromator crystal

Dimension of 1st crystal WxHxL: 50x55x120mm³

Case	K	Add. filter [mm]	H [μrad]	Energy [keV]	Foot- print [mm]	Total heat [W]	Power density [W/mm ²]	T _{Max} [K]	Total Slope _M [μrad]	Calc Param (*)
A	6.08		400	10	8.8x12.4	464	4.37	160	+26	6000/2000/90
B	4.8		400	10	8.8x12.4	433	4.14	154	+19	6000/2000/90
C1	6.08	(C1.3Be0.3)	100	40	2.2x50	267	2.64	114	+0.4	6000/2000/90
C2	6.08	(C1.3Be0.3)	100	40	2.2x50	267	2.64	90	+1.6	6000/6000/77
D	4.8		200	10	4.4x12.4	217	4.14	121	+0.8	6000/2000/90
E	6.08	C2.0	200	40	4.4x50	442	2.2	123	+3.3	6000/2000/90

(*) Convect. Heat Transfer coeff. [W/m²K] / Heat Conductance Si/Cu [W/m²K] / T_{IN2} [K]

The pre filter was 0.4mm diamond plus 0.3mm Be, except the case marked with brackets in column "Add. filter".

The table shows that horizontal apertures of 200 μrad produce total slope error smaller than case I (40keV, +5μrad) considered in the CDR, section 4.3.2, therefore, it is expected that the change in the vertical divergence of the beam and the loss of flux is acceptable.

5.3 Estimation of the optical characteristics of the collimating mirror

5.3.1 Slope error

The acceptable slope error of the collimating mirror can be estimated analogous to the slope error of a focusing optics. The focal spot size of the focusing optics then corresponds to the source size that has to be imaged to infinity by the mirror. The source

is magnified by two times the slope error and the distance between mirror and image/source.

The maximum RMS slope error μ to blow up the source image not more than 10% is then: $\mu < s/4r$ with s : source size, and r : distance between source and mirror.

For a K value of 6.08 and at 40keV the vertical RMS-source size is (calculated with SPECTRA): $s = 32\mu\text{m}$, together with a source-mirror distance of $d = 20\text{m}$ we get:

$$\mu < 0.4 \mu\text{rad}.$$

This is a very tight condition. For the typical slope error of $1.5\mu\text{rad}$ that can be achieved for mirrors of that size the spot is blown up by 40%. This seems to be acceptable.

5.3.2 Surface roughness

A criterion describing the reflecting efficiency of an optical element is the "Strehl-criterion". A value of $I=0.8I_0$ is assumed to describe a diffraction limited optic. At a mirror angle of 2mrad and at an energy of 40keV and with

$$I = I_0 e^{-\left(\frac{4\pi\theta\sigma}{\lambda}\right)^2}, \text{ we get the following RMS surface roughness:}$$

I/I_0 RMS roughness [nm]

0.9 0.4

0.85 0.5

0.79 0.6

A RMS mirror roughness of better than 0.6 nm should therefore be achieved.

6 Vertical beam positions and beam sizes

With the preliminary values given in section 3 we get the following vertical positions in mm for the beam center relative to the orbit (1400mm).

Element	ID	Mirror	Mono	End OE	Station 1	Station 2
Distance [m]	0	20	23	28	32	35
V shift [mm] Un-mirrored	0	0	0	20	20	20
V shift [mm] mirrored	0	0	12	52	68	80
V shift [mm] KB 20keV ML 0.3nm	0	0	0	20	72.5	
V shift [mm] Mirror+KB 20keV ML 0.3nm	0	0	12	52	120.5	
V shift [mm] KB 40keV ML 0.3nm	0	0	0	20		47.5
V shift [mm] Mirror+KB 40keV ML 0.3nm	0	0	12	52		107.5

Under operational conditions the maximum divergence of the beam will be HxV 400x125 μ rad and typically 200x125 μ rad. For initial alignment the maximum achievable opening is 1400x350 μ rad.

7 Preliminary Floor layout

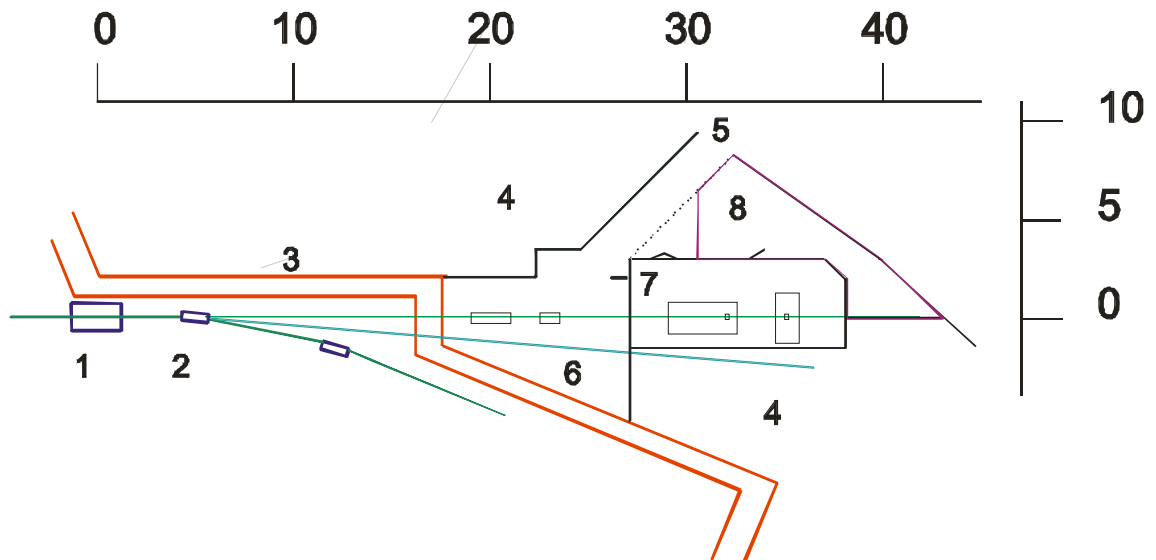


Figure 7.1: Preliminary layout of the hutches, distances given in meters. 1: ID, 2: next bending magnet, 3: shield wall, 4: neighboring beamline, 5: access to optics hatch, 6: optics hatch, 7: experimental hatch with HP and PD station, 8: control area.

The total floor space allocated to the beamline is 110m². Both neighboring bending magnet beam ports must be kept open for later use. The two beams from ID and downstream BM exit the shield wall with a separation of about 1050mm. Since lateral space in the OE is very tight the optics hatch will be shared between both beamlines.

The liquid nitrogen cooling system will be placed on top of the roof of the optics hatch.

8 References

A. Chumakov, R. Rueffer, O. Leupold, J. P. Celse, K. Martel, M. Rossat, W. K. Lee. *Performance of a cryogenic silicon monochromator under extreme heat load*. J. Synchrotron Rad. 11 (2004) 132-141.

V. O. Kostroun. *Identification of "spurious" reflections in "channel-cut" monochromators*. Nuclear Instruments and Methods 172 (1980) 243-247.

http://www.cells.es/Beamlines/HRPD/Laue_spots_ccm/index

G. Tajiri, W. K. Lee, P. Fernandez, D. Mills, L. Assoufid, F. Amirouche. *Nonlinear thermal-distortion predictions of a silicon monochromator using the finite element method*. J. Synchrotron Rad. 8 (2001) 1140-1148.

L. Zhang, W. K. Lee, M. Wulff, L. Eybert. *The performance of a cryogenically cooled monochromator for an in-vacuum undulator beamline*. J. Synchrotron Rad. 10 (2003) 313-310.